

RESEARCH

Open Access



Nur77 ameliorates cyclophosphamide-induced ovarian insufficiency in mice by inhibiting oxidative damage and cell senescence

Ying Yao^{1†}, Bin Wang^{2,3†}, Kaihua Yu¹, Ji Song^{2,3}, Liyan Wang^{2,3}, Xia Yang^{2,3}, Xuehong Zhang^{2,3}, Yulan Li^{4,5*} and Xiaoling Ma^{2,3,5*}

Abstract

Premature ovarian failure (POF) is among the primary causes of ovarian dysfunction that severely affects women's physical and mental health. The main purpose of this study was to explore the expression level of Nerve growth factor-induced protein B (Nur77/NR4A1) in cyclophosphamide (CTX)-induced POF. We then tested whether Nur77 can exert a protective effect after CTX treatment and investigated the mechanism of Nur77's role during ovarian injury. CTX promotes follicular atresia by inducing redox imbalance, apoptosis, and senescence, thereby causing direct toxicity to gonads. Additionally, CTX decreases ovarian reserve consumption by stimulating the excessive activation of primordial follicles. Nur77 can be stimulated by oxidative stress, DNA damage, metabolism, inflammation, etc. However, its relationship with POF remains unelucidated. We here found that Nur77 is expressed at low levels in POF ovaries. Therefore, Nur77 was identified as a regulator of ovarian injury and follicular development. According to the results, Nur77 overexpression alleviated redox imbalances, reduced cell senescence and apoptosis, and improved follicular reserve. Nur77 protects ovarian function by restoring disordered sex hormone levels and estrus cycles and promoting follicle growth and development at all levels. Moreover, the rapamycin protein kinase (AKT)/mammalian target of the rapamycin (mTOR) is a crucial regulator of the primordial follicle pool and follicular development. A relationship was observed between Nur77 and AKT through string and molecular docking. Experiments confirmed the involvement of the AKT/mTOR signaling pathway in the regulatory role of Nur77 in ovarian function. Thus, Nur77 is a critical target for POF prevention and treatment.

Keywords Nur77, Granulosa cells, CTX, POF, Aging, Apoptosis

[†]Ying Yao and Bin Wang contributed equally to this work.

*Correspondence:

Yulan Li

liyul@lzu.edu.cn

Xiaoling Ma

maxl2005@163.com

¹The First School of Clinical Medicine, Lanzhou University, Lanzhou, China

²Reproductive Medicine Center, The First Hospital of Lanzhou University, Lanzhou, China

³Key Laboratory for Reproductive Medicine and Embryo of Gansu, Lanzhou, China

⁴Department of Anesthesiology, The First Hospital of Lanzhou University, Lanzhou, China

⁵No. 1, Donggang West Road, Chengguan District, Lanzhou City, Gansu Province, China



Introduction

Ovarian dysfunction is often characterized by diminished oocyte quantity and quality, as well as a reduced ovarian reserve, which can stem from various causes. Premature ovarian failure (POF) affects 1–5% of women under 40 and is a leading cause of human infertility [1]. One major contributor to POF is gonadal damage resulting from radiation, chemotherapy, or surgical procedures. Although significant advancements in biomedicine have improved early tumor detection and treatment, benefiting survival rates, female children and cancer survivors of childbearing age represent a unique group. For their long-term physical and mental health, gynecological examinations and fertility counseling following cancer treatment are particularly important [2].

Cyclophosphamide (CTX) is a widely used chemotherapy drug for treating various cancers, including breast and ovarian cancer, and leukemia [3–5], as well as other conditions such as systemic sclerosis, aplastic anemia, and lupus nephritis [6–8]. Being a non-cell cycle-specific drug, CTX's active metabolites bind to DNA, causing double-strand breaks that inhibit DNA replication and protein synthesis, leading to effective anticancer results. However, this indiscriminate action also damages normal cells, particularly affecting ovarian function [9]. This damage persists even after the tumor tissue is effectively controlled. CTX is known for its gonadotoxic effects, leading to ovarian dysfunction and POF [10] by directly damaging the ovaries and indirectly promoting the reduction in reserve follicles by stimulating the excessive activation of primordial follicles, a process referred to as "burnout" [11]. Although various fertility preservation strategies, such as cryopreservation of ovarian tissue, oocytes, or embryos, have been proposed for use in female cancer patients [12], they may not be feasible for all patients. In some cases, the viability of cryopreserved germ cells cannot be determined, and thus, pregnancy cannot be guaranteed. Thus, the success of these methods is uncertain. Thus, further investigation into the molecular mechanisms and signaling pathways involved in chemotherapy-induced ovarian damage is necessary to develop new fertility preservation methods.

The exact mechanism underlying CTX-induced ovarian damage is complex, intricate, and not entirely understood. CTX reduces antioxidant enzyme production, promotes oxidative stress and inflammation, and disrupts the ovarian microenvironment, leading to an imbalance between pro-apoptotic and anti-apoptotic genes. This disruption ultimately results in germ cell apoptosis and follicular atresia [13–15]. Additionally, CTX can adversely impact ovarian reserve by activating multiple targets in dormant primordial follicles, such as forkhead box O3a (FOXO3a), via phosphorylated Akt [16]. Recent research suggests that ovarian cell senescence plays a

significant role in CTX-induced POF and highlights the potential for targeting senescent cells as a strategy to prevent CTX-induced ovarian damage, which occurs through various mechanisms [17]. Given the complexity of CTX's effects, drugs or molecules can target multiple pathways to protect the ovaries from damage caused by alkylating agents such as CTX.

Nerve growth factor-induced protein B (Nur77, also known as NR4A1), is part of the nuclear hormone receptor NR4A subfamily and functions as an early response gene involved in regulating various pathological and physiological processes, including oxidative stress, inflammation, metabolism, cell cycle, and apoptosis [18–21]. Oxidative stress damages the Nur77-Silent mating type information regulation 2 homolog-1 (Sirt1) axis, causing a decline in homeostasis during aging, which then induces additional oxidative stress and offers positive feedback for premature aging by further reducing Nur77 expression [22]. Low Nur77 levels accelerate aging. Interestingly, in the Parkinson's disease cell model, high Nur77 expression attenuates the inflammatory response and oxidative stress by inhibiting recombinant Inhibitory Subunit Of NF Kappa B Alpha (IkB- α) phosphorylation [23]. In another study with a similar conclusion, Nur77 alleviated endothelial dysfunction-related cardiovascular diseases by upregulating nitric oxide (NO) and superoxide dismutase (SOD), an antioxidant enzyme, in the vascular endothelium [24]. Thus, Nur77 plays a crucial regulatory role in cell function from many aspects. Despite the critical role of oxidative stress, cell senescence, and apoptosis in CTX-induced POF, the Nur77 expression status in POF and whether Nur77 plays a regulatory role in POF occurrence and development have not been explored.

We here first verified that CTX successfully induced POF models, which exhibited reduced Nur77 expression. Subsequent animal experiments suggested that Nur77 regulates POF, as Nur77 overexpression improved follicle count and corrected abnormal sex hormone levels associated with ovarian dysfunction. This protective effect of Nur77 involves inhibiting the activation of the rapamycin protein kinase (AKT)/mammalian target of the rapamycin (mTOR) signaling pathway, regulating redox imbalance, and decelerating germ cell senescence and apoptosis.

Materials and methods

Animals

Female C57BL/6 mice (age: 6–8 weeks) were purchased from the Lanzhou Veterinary Research Institute and housed under specific pathogen-free conditions, with controlled temperature ($22^{\circ}\text{C} \pm 1^{\circ}\text{C}$) and humidity (60% $\pm 10\%$). The mice had unrestricted access to water and food during a 12-h light-dark cycle. The Animal Ethics

Committee of the First Hospital of Lanzhou University approved all animal experiments (experimental protocol number: LDYYLL2024-346).

Animal treatment

First, vaginal smears of all female C57BL/6 mice (age: 6–8 weeks) were prepared to observe their estrus cycles. Subsequently, mice with normal estrus cycles were randomly assigned to 4 groups: a control group, a CTX group, an adeno-associated virus negative control group (AAV-NC), and an adeno-associated virus Nur77 group (AAV-Nur77). The treatment protocol involved establishing a POF mouse model through a single intraperitoneal injection of CTX (75 mg/kg; MCE, China), after balancing the mice for 1 week. Nur77 overexpression was achieved by administering AAV (Genechem Co., Ltd., China) according to the manufacturer's protocol. The control group received no treatment, whereas the AAV-NC and AAV-Nur77 groups were injected with 1.5 mg/kg of the virus. The day of *in situ* virus injection was designated as Day 1, with a continuous observation period of 4 weeks. Because the normal estrus cycle of the mouse is 4–5 days, daily vaginal smears were performed from Day 20 post-transfection for 9 consecutive days until sampling (Fig. 1A). The *in situ* virus injection adhered to strict aseptic techniques. First, the mice were anesthetized with 1% pentobarbital sodium, and their lower backs were shaved and disinfected with 75% alcohol. A 0.5-cm incision was made on the bilateral lower back to access the ovaries. The tissue was carefully separated using tissue tweezers, and the ovary was gently exposed. The virus was injected slowly into the ovary over approximately 3 min by using a 5-μL syringe, resulting in the swelling of the ovarian capsule. After the mice were injected, the site was compressed with sterile gauze for 2–3 min for hemostasis. The ovary was repositioned, and the incision was sutured. After 4 weeks of AAV-Nur77 treatment, all animals were sacrificed under anesthesia for further experimental analysis.

Vaginal smears and estrus cycle determination

Vaginal smears were performed daily at 9:00 a.m. for 9 consecutive days following Nur77 treatment to assess the estrus cycle. The process involved moistening a cotton swab with normal saline, gently rotating it in the vagina, and then applying the sample to a slide. Next, the isolated cells were stained with hematoxylin and eosin (H&E) to identify the various stages of the estrus cycle, which are characterized as follows: proestrus, characterized by predominantly irregularly shaped nucleated epithelial cells, with few leukocytes and keratinized epithelial cells; estrus, almost entirely composed of lamellar anucleated keratinized cells; metestrus, characterized by a small number of non-nucleated keratinized epithelial

cells, with leukocytes comprising the majority of cells; and diestrus, characterized by crinkled epithelial cells and numerous leukocytes.

Body weight and ovarian index

Daily observations were made to assess the activity and fur condition of the mice. Their body weights were recorded regularly until the experiment concluded. At the end of the study, the four groups of mice were euthanized. The ovaries were then excised for measurement and photography, and the ovarian index was calculated using the formula: ovarian weight (g)/body weight (g). This index serves as an indicator of ovarian development and function. Following this, the ovarian tissue was either fixed in 4% paraformaldehyde or stored at –80 °C for later cryopreservation.

H&E staining and Masson's trichrome staining

The ovaries of the mice were collected and fixed in 4% paraformaldehyde. After the ovaries were fixed, they were embedded in paraffin, sectioned into 5-μm slices, and stained with H&E. After staining was completed, follicles were classified and counted to evaluate the impact of Nur77. Briefly, ovaries were serially sectioned every 5 μm, with every tenth section being stained with H&E. The follicles were classified based on the Pederson standard. The number of follicles at each stage was estimated by counting the follicles in every tenth section and multiplying the total count by a correction factor of 10 to represent the entire ovary [25].

Enzyme-linked immunosorbent assay (ELISA)

According to the instructions of the mouse E2, AMH and FSH ELISA kit (Fankew, China), serum samples from mice in each group were collected. Then, 50 μL of HRP detection antibody was added to the wells of the samples to be tested and the wells of the standard, incubated at 37 °C for 1 h, topped up with washing solution, shaken for 30 s and washed 5 times. Fifty microlitres of substrates A and B were added to each well, incubated at 37 °C for 10 min, and the OD value was detected at 450 nm. The actual concentration of the sample was calculated according to the standard curve.

Malondialdehyde and superoxide dismutase assays

Ovarian tissue was lysed using lysis buffer for the Western and IP Kit (Boster, China) or using PBS and kept in an ice bath. The tissues were homogenized through brief oscillation. The homogenates were centrifuged at 2000 ×g for 10 min at 4 °C, and the supernatants were collected for further experiments. Protein concentrations of the supernatants were determined using the Bicinchoninic Acid (BCA) Protein Assay Kit (Thermo, USA). Malondialdehyde (MDA) levels were measured using

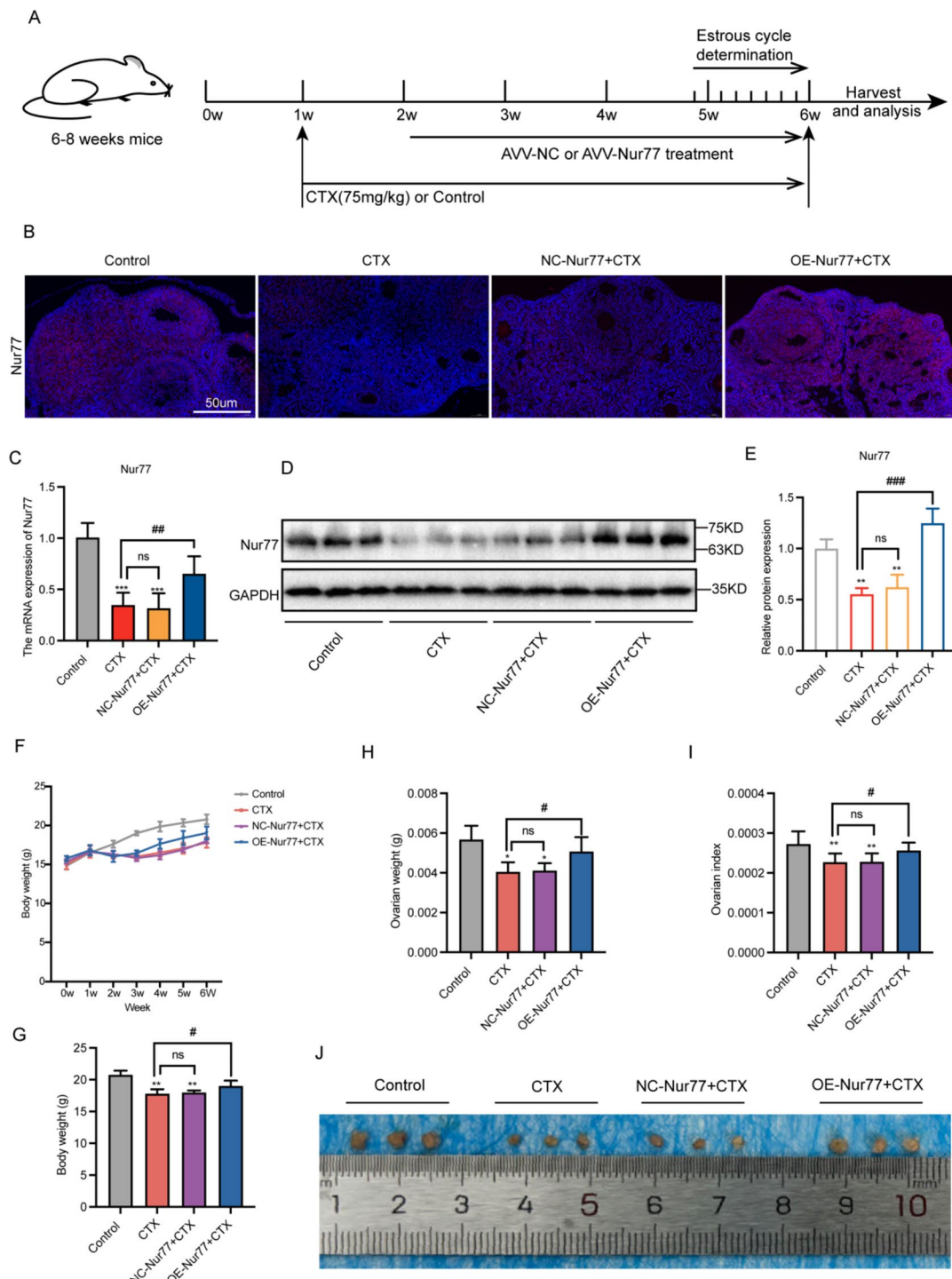


Fig. 1 Nur77 increased the POF mice's ovarian index. **(A)** Treatment timeline of Nur77 in CTX mice. **(B)** Immunofluorescence staining was performed to detect the localization and expression of Nur77 in the ovarian tissues of each group after the overexpression of Nur77. Scale bar: 50 μm. **(C)** The mRNA expressions of Nur77 in each group after the overexpression of Nur77. **(D)** & **(E)** The protein expressions of Nur77 in each group after the overexpression of Nur77. **(F)** The changes in the body weight of mice in each group after the overexpression of Nur77. **(G)** The comparison of the body weights of mice in each group at the end of the study. **(H)** & **(I)** Ovarian weight and ovarian index of mice in each group after the overexpression of Nur77. **(J)** Ovarian images of mice in each group after the overexpression of Nur77. Error bars, mean ± SEM. n = 6–8/group. *P < 0.05, **P < 0.01 versus the control group. ns, not significant; #P < 0.05, ##P < 0.01, ###P < 0.001 versus the CTX group

the Lipid Peroxidation MDA Assay Kit (Solarbio, China) and calculated using a standard curve in accordance with the manufacturer's instructions. SOD activity was determined using the Toal SOD Assay Kit with WST-8 (Beyotime, China) and calculated according to the manufacturer's instructions. All the experiments were repeated independently three times for statistical reliability.

Western blot analysis

Ovaries were lysed on ice using RIPA buffer (Boster, China) and centrifuged at 4 °C and 12,000 r for 15 min. Proteins were separated by 10% SDS-PAGE and transferred to PVDF membranes (Millipore, USA). The PVDF membrane was blocked in TBST containing 5% skim milk for 2 h. Following this, membranes were incubated with rabbit polyclonal anti-Nur77 (1:1,000 dilution; Abcam), rabbit polyclonal anti-p16 (1:1,000 dilution; Abcam), rabbit polyclonal anti-p21 antibodies (1:2,000 dilution; Proteintech), rabbit polyclonal anti-Parkin antibodies (1:1,000 dilution; Abcam) and mouse monoclonal anti-PINK1 antibodies (1:500 dilution; Abcam) at 4 °C. And then the HRP-conjugated secondary antibody. An ECL detection kit (Boster, China) was used for visualization. Protein bands were visualized using the Automatic Gel Imaging System (Bio-Rad, USA). ImageJ was used to determine significant differences in the protein expression.

Immunofluorescence (IF)

Following fixation, the slides were permeabilized using 0.1% Triton-X for 30 min. Subsequently, the slides were placed in a blocking buffer containing 10% goat serum and 1% BSA in PBS for 1 h. Next, the sections were incubated with primary antibody against Nur77 (1:100 dilution; Abcam), P16 (1:100 dilution; Proteintech), H2AX (1:100 dilution; MCE), or LC3 (1:200 dilution; Proteintech) at 4 °C. After washing with PBS, they were incubated with secondary antibody for 1 h at room temperature and then stained with DAPI (Solarbio, China) solution for 10 min.

Terminal-deoxynucleotidyl transferase mediated nick end labeling (TUNEL)

A TUNEL cell apoptosis detection kit (Servicebio, China) was used to examine apoptosis in ovarian sections. The analysis was performed according to the manufacturer's instructions. In brief, after being permeabilized, the sample was incubated with the TUNEL detection solution. The nucleus was labeled with DAPI. Finally, the samples were analyzed by fluorescence microscopy (Nikon, Japan).

Real-time qPCR

Total RNA containing cells and ovary tissue were extracted by Trizol method. The RNA was reverse-transcribed according to the instructions of kit (Tiangen, China,). RT-qPCR was implemented using TB Green® Premix (Takara, Japan) on a ABI applied biosystems. The primers used were as following:

| | Forward | Reverse |
|---------|--------------------------|------------------------------|
| Nur77 | AGCTTGGGTGTTGATGTTCC | TAAAGGCACATGGGTGA CAG |
| p53 | TGCTCCGATGGTGATGGC | TTCCAGATACTCGGGATAC AAATT |
| p21 | GGGACAAGAGGCCAGTACT | CAATCTGCGCTGGAGTGA |
| p16 | GGCTCTGCTCTGGGATTGG | ATCGCGATATTGCGTTCC |
| H2AX | TTGATTGCCGGGCTTAGAGG | CTGCGCAGGTATAAGACTC |
| Bax | GCCTTTGCTACAGGGTT CAT | TATTGCTGTCCAGTTCATC TCCA |
| Bcl2 | TGACTTCTCGTCGCTACCGT | CCTGAAGAGTTCCAC CACC |
| β-actin | GTGACGTTGACATCCGTAAGA | GTAACAGTCGCCTAGAA GCAC |

KEGG pathway enrichment analysis

We performed pathway enrichment analysis using the microarray data from the GEO database (GSE128240) involving those mice with CTX-induced POF [26]. Differential gene expression analysis was performed using the Limma package, with P2 as the screening standard. The GSEA function in the clusterProfiler package was employed to conduct pathway enrichment, focusing on the KEGG pathway. Finally, the results, including the normalized enrichment score (NES) and adjusted p-value of the PI3K-AKT-MTOR pathway, were visualized using ggplot2.

Network construction and molecular docking

The protein–protein interaction (PPI) network for Nur77 was constructed using the STRING database and visualized using Cytoscape 3.8 for the network analysis. Additionally, molecular docking was performed using Zdock3.0.2 and the protein models Nur77 (PDB ID: 2QW4) and AKT (PDB ID: 1H10). Nur77 and AKT were selected as the receptor protein and ligand-protein, respectively. Protein pretreatment, including deletion of water molecules and excess ligands, and hydrogen atom addition, was completed using PyMol 2.5. The model with the lowest binding energy was selected as the best docking model, and PyMOL was used for visualization.

Statistical analysis

All experiments were performed at least three times. The data were analyzed by SPSS 25.0 software (Chicago, USA) and are presented as the mean±SD. Comparisons among three or more groups were performed with one-way

analysis of variance (ANOVA). The results were followed by the least significant difference (LSD) test between the two groups and Tamhane's T2 test was performed when the variance was unequal. All tests were two-tailed and $p < 0.05$ was considered as statistically significant.

Results

Reduced Nur77 expression in POF mouse ovaries

To determine Nur77 expressions in POF and accurately evaluate their effect on ovarian function in subsequent experiments, the effect of CTX intraperitoneal injection on the POF model was verified. Compared with the control group, the CTX group exhibited abnormal sex hormone levels (Anti-Müllerian Hormone, AMH and Estradiol, E₂ levels decreased, whereas Follicle-stimulating hormone, FSH levels increased) (Fig. 2A). Moreover, the number of primordial follicles and antral follicles, and formation of corpus luteum significantly reduced in the CTX group, whereas the number of atretic follicles increased (Fig. 2B and C). Clinically, ovarian function is often evaluated on the basis of sex hormone levels and the number of follicles. Therefore, our research focused on the decline in ovarian function based on these indicators. Subsequently, the Nur77 expression was detected through western blotting and immunofluorescence (Fig. 2D–F). Finally, Nur77 expression significantly decreased in the CTX group. Nur77 regulates various ovarian function-related stress responses, such as oxidative stress, apoptosis, and aging [27–29]. Consequently, we assumed that Nur77 plays a protective role in POF occurrence and development and conducted subsequent experiments.

Nur77 increases the ovarian index in POF mice

To evaluate the degree of CTX-induced ovarian damage and the protective effect of Nur77, an adeno-associated virus was used to overexpress Nur77. Figure 1A presents the timeline diagram for the Nur77 intervention. After all mice were balanced for 1 week, the control group received no treatment. The mice in the CTX group were intraperitoneally injected 75 mg/kg CTX. The AAV-NC group received an in situ injection at 1.5 mg/kg 1 week after the CTX treatment. In the AAV-Nur77 group, AAV-Nur77 was injected in situ at the same dose. The day of in situ virus injection was regarded as D1 day of treatment, with a continuous observation period of 4 weeks until sampling (Fig. 1A). Immunofluorescence results revealed that the red fluorescence area of the ovaries in the OE-Nur77+CTX group, which indicated the Nur77 expression, was considerably larger than that in the CTX and NC-Nur77+CTX groups (Fig. 1B). Additionally, the gene and protein detection results supported this finding. Nur77 was successfully overexpressed in the POF model (Fig. 1C–E). Throughout the experiment, we measured

and recorded the mouse weight weekly (Fig. 1F–G), as well as the weight of the ovaries at the end of the experiment (Fig. 1H). The ovarian index was also calculated for each group (Fig. 1I). The control group's weight gradually increased. The body weight, ovarian weight, and ovarian index significantly decreased in the CTX and NC-Nur77+CTX groups. However, Nur77 overexpression effectively reversed these changes. To present changes in mouse ovaries more intuitively, one ovary was randomly selected from three mice from each group for photography. The results revealed that Nur77 overexpression significantly improved CTX-induced reduction in the mouse ovarian volume (Fig. 1J).

Nur77 improves sex hormone disorders and abnormal estrus cycles in POF mice

To further evaluate the degree of CTX-induced ovarian damage and the protective effect of Nur77, the sex hormone levels and estrus cycles of mice in each group were observed. Compared with the control group, AMH expression decreased in the CTX-treated mice. However, the Nur77 intervention reversed this decline (Fig. 3A). Moreover, CTX-induced ovarian damage was accompanied by an increase in serum FSH levels, with a decrease in E₂ levels. Notably, the Nur77 treatment reversed the levels of these two hormones, even bringing their levels close to normal levels (Fig. 3A). Estrus cycles in mice were similar to the periodic regulation of the human menstrual cycle by sex hormone levels. Given that mice typically have a 4–5 day estrus cycle, daily vaginal smears of the mice were prepared for the final 9 days of the Nur77 intervention until the samples were collected (Fig. 1A). The estrus cycle of each group of mice was evaluated by microscopically observing the main cell types in the vaginal smears. Fig. 3B presents a classic smear of the four stages of the estrus cycle (proestrus, estrus, diestrus, and metestrus). The CTX-induced estrus cycle disorder in mice was corrected through Nur77 overexpression, which resulted in an "N"-like cycle curve (Fig. 3C). The Nur77-treated mice exhibited more estrus (E) than metestrus, anestrus (M/D), or proestrus (P) cycle (Fig. 3D).

Nur77 improves ovarian follicular development in POF mice

To investigate the effect of CTX on follicular development in POF mice and Nur77 regulation, pathological sections of the ovaries from each group of mice were stained with H&E and observed. The number of follicles was counted at each stage. According to studies, the number of primordial follicles in the mice treated with CTX for 7 days started decreasing. The number decreased more significantly after CTX treatment for 2 weeks. The depletion of primordial follicles lasted for more than 20 days [1]. Therefore, in this study, Nur77

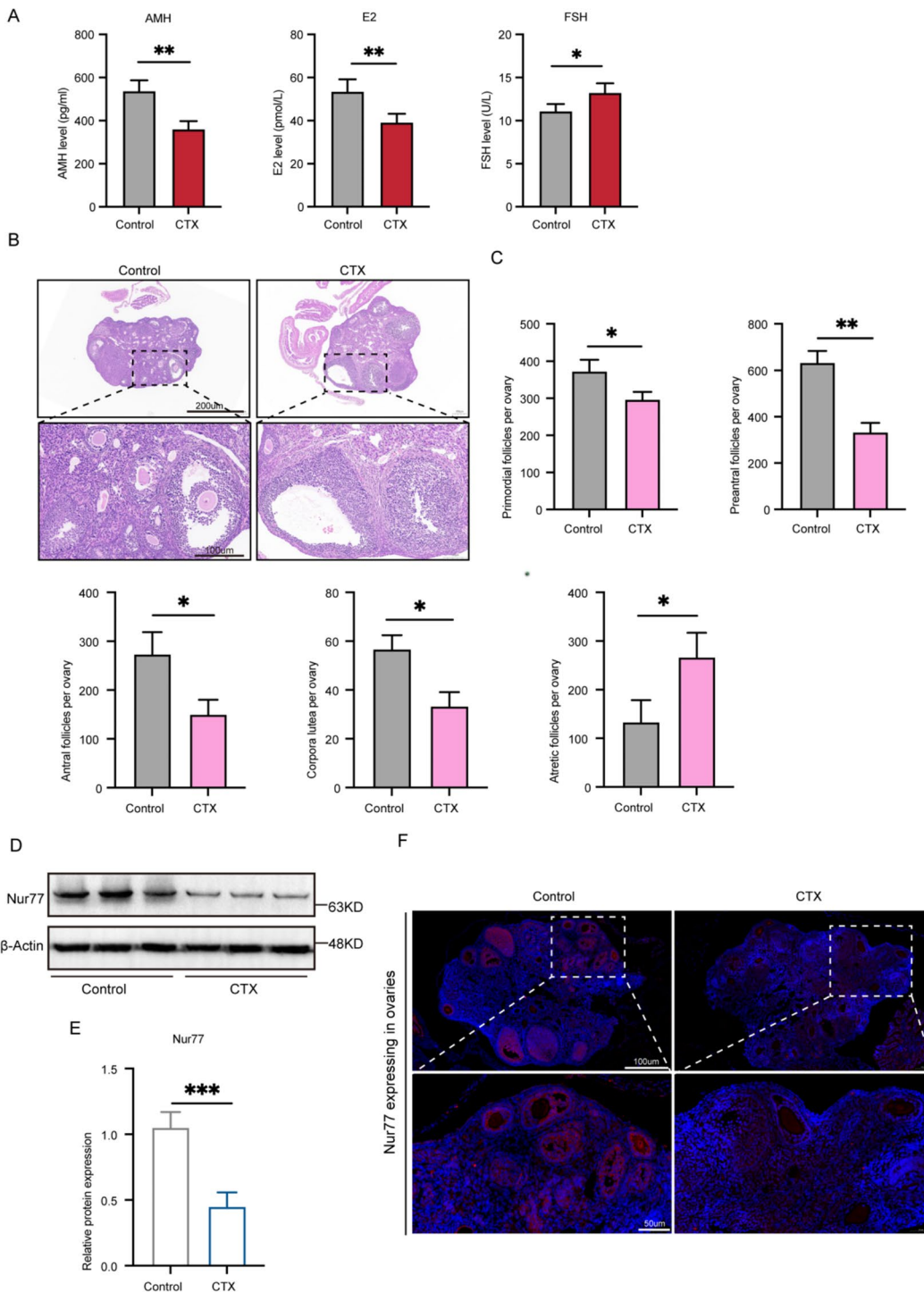


Fig. 2 Reduced Nur77 expression in POF mice's ovaries. **(A)** Comparison of serum sex hormones AMH, E₂, and FSH between the control and CTX groups. **(B)** & **(C)** Representative images of H&E staining of ovaries tissues and follicle count in the control and CTX groups. **(D)** & **(E)** The protein expressions of Nur77 between the control and CTX groups. **(F)** Immunofluorescence staining was performed to detect the localization and expression of Nur77 in the ovarian tissues of the control and CTX groups. Scale bar = 200, 100, and 50 μ m. Error bars, mean \pm SEM. $n=6-8/\text{group}$. * $P<0.05$, ** $P<0.01$, *** $P<0.001$ versus the control group

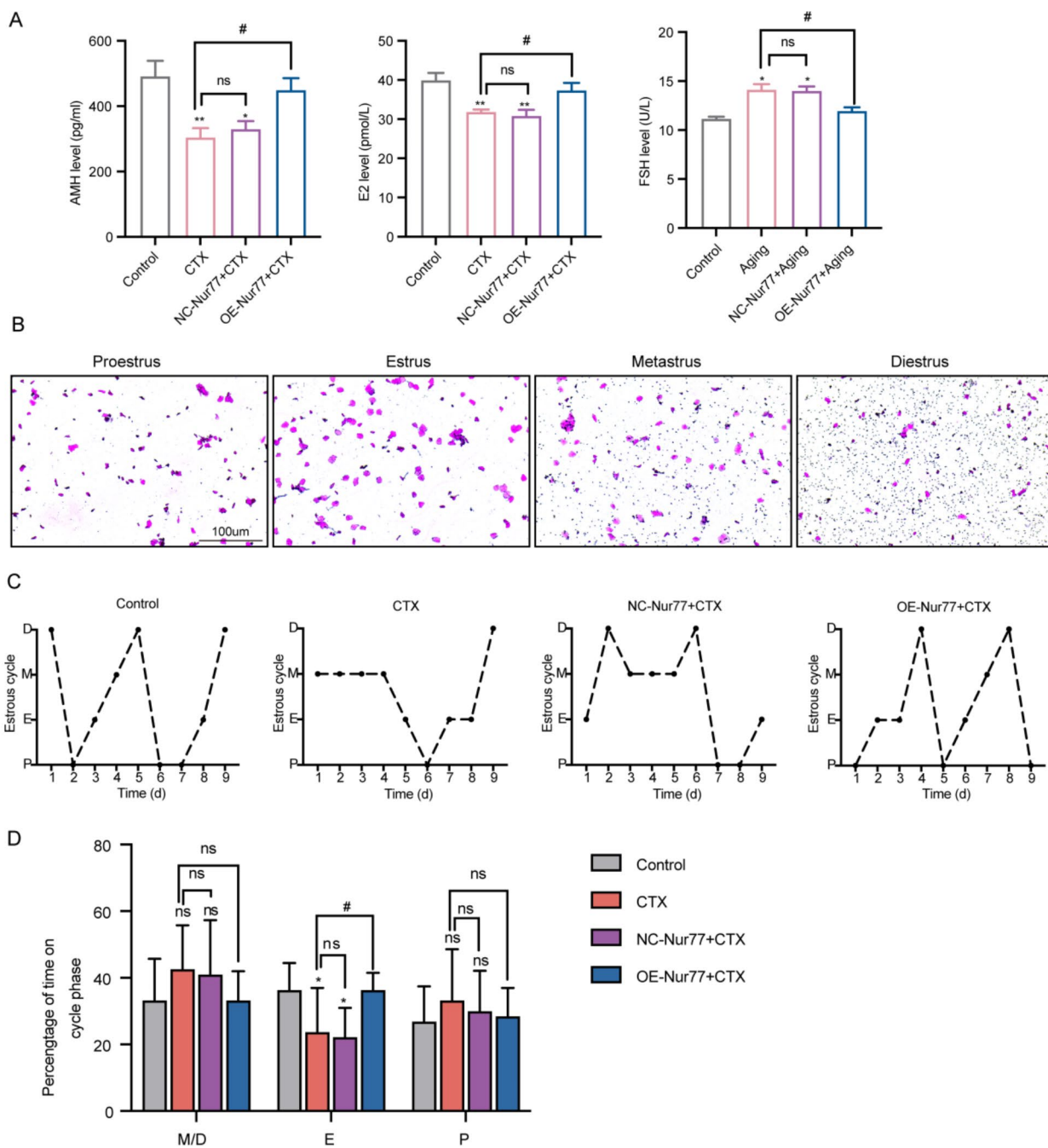


Fig. 3 Nur77 improves sex hormone disorders and abnormal estrous cycles in POF mice. **(A)** Comparison of serum sex hormones AMH, E₂, and FSH in each group after the overexpression of Nur77. **(B)** Characteristics of vaginal smears in different stages of the estrous cycle in mice. Scale bar: 100 μm. **(C)** Representative estrous cycles (proestrus, estrus, metestrus, and diestrus). **(D)** Quantitative analysis of time on the cycle phase in 9 days. Error bars, mean ± SEM. n = 6–8/group. ns, not significant; *P < 0.05, **P < 0.01 versus the control group. #P < 0.05 versus the CTX group

overexpression was performed at 7 days after CTX treatment, and the final effect was observed after 4 weeks of continuous treatment (Fig. 1A). H&E-stained ovaries revealed that Nur77 overexpression alleviated CTX-induced ovarian damage and promoted normal follicular

development (Fig. 4A). A statistical analysis of various follicle types unveiled that the number of primordial follicles, preantral follicles, and antral follicles decreased in the ovaries of the CTX group, whereas that of atretic follicles increased significantly. Nur77 overexpression

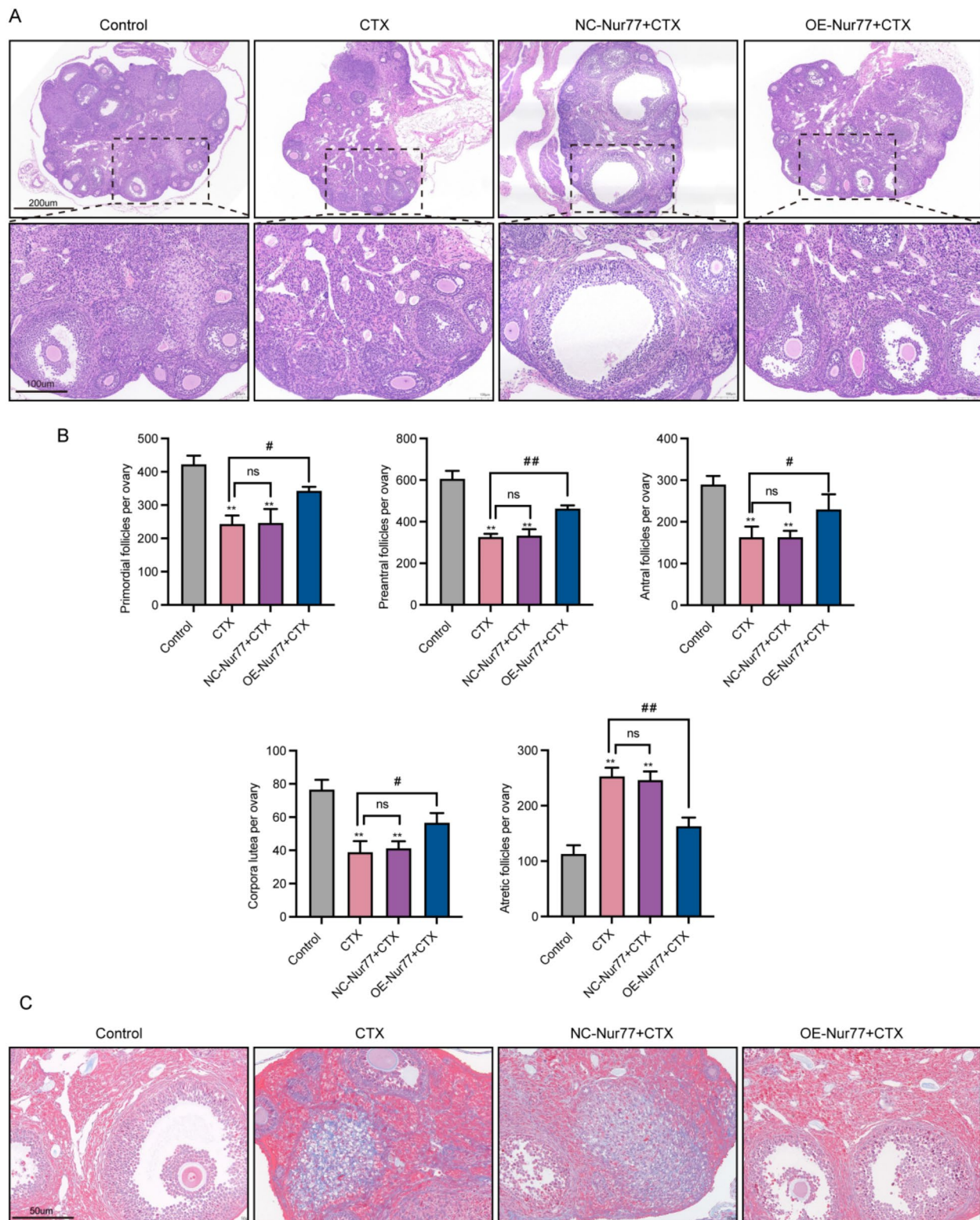


Fig. 4 Nur77 improves follicular development in the ovaries of POF mice. **(A)** & **(B)** Representative images of H&E staining of ovaries tissues, and follicle count in each group after the overexpression of Nur77. Scale bar: 200 and 100 μ m. **(C)** Representative images of Masson staining of the ovaries tissues in each group after the overexpression of Nur77. Scale bar: 50 μ m. Error bars, mean \pm SEM. $n=6-8/\text{group}$. * $P<0.05$, ** $P<0.01$ versus the control group. ns, not significant; # $P<0.05$, ## $P<0.01$ versus the CTX group

reversed this adverse trend (Fig. 4B). Moreover, the CTX group demonstrated a reduction in the formation of corpus luteum compared with the control group, thereby suggesting that CTX-induced ovarian injury led to ovulation disorders, which the Nur77 intervention also alleviated (Fig. 4B). CTX-induced ovarian damage can be complicated by ovarian fibrosis [30]. The same fibrosis was observed in the CTX group, and Nur77 overexpression reduced the fibrosis of CTX ovaries. This may also be the reason for the stimulation and enhancement of ovulation and ovarian function by Nur77 (Fig. 4C).

Nur77 reduces oxidative stress and apoptosis in the ovaries of POF mice

Active CTX metabolites, such as acrolein, lead to the consumption of several antioxidant enzymes and the production of several pro-oxidants. This places germ cells in a microenvironment of oxidative stress, which further results in apoptosis, follicular atresia, and ovarian function decline [31, 32]. The level of SOD, an anti-oxidant enzyme, significantly decreased in the ovarian tissue of the CTX group, whereas that of the lipid peroxidation index MDA significantly increased. Nur77 overexpression significantly reversed the redox imbalance (Fig. 5A). As expected, gene detection revealed that CTX decreased the expression of the anti-apoptotic gene Bcl2, whereas increased the expression of the pro-apoptotic gene Bax (Fig. 5B). This finding was consistent with the protein results (Fig. 5C and D). However, Nur77 overexpression effectively prevented the pro-apoptotic process caused by the Bcl2 and Bax imbalance. Furthermore, we performed the TUNEL assay to more intuitively evaluate the impact of Nur77 on ovarian apoptosis in POF mice. Of note, CTX stimulation significantly increased apoptosis (TUNEL-positive cells increased). However, the Nur77 intervention significantly reduced TUNEL staining (Fig. 5E and F).

Nur77 attenuates ovarian aging in POF mice

Exposure to reactive oxygen species (ROS) can trigger cell senescence, a crucial pathogenic factor for POF [17]. A significant aging phenotype has been observed in the ovarian granulosa cells of POF patients and in CTX-pretreated granulosa cells, which is positive for galactosidase staining [33]. In the ovaries of CTX-induced POF mice, the cell senescence markers p53, p21, p16, and H2AX were significantly upregulated [17]. Cell senescence is among the major causes of CTX-induced ovarian damage. Our study again supports this conclusion. In the ovaries of the CTX-treated mice, the expressions of p53, p21, p16, and H2AX genes (Fig. 6A) and proteins (Fig. 6B-C) significantly increased. The results of immunofluorescence staining of p16 and H2AX increased the credibility of the results (Fig. 6D). Importantly, Nur77

was overexpressed, but the expression of these aging indicators was significantly reduced. Thus, Nur77 was suggested to improve the ovarian function of POF mice by reducing cell senescence.

Nur77 improves ovarian function through the Akt/mTOR pathway

In this study, Nur77 promoted follicular development and improved ovarian function by regulating the redox imbalance and inhibiting apoptosis and senescence. However, the underlying mechanism remains unclear. Notably, upregulation of the Akt/mTOR axis is associated with follicular depletion and ovarian dysfunction caused by excessively activated primordial follicles [34]. In the KEGG pathway enrichment analysis of the dataset (GSE128240), the enrichment score of the PI3K-AKT-mTOR pathway was 1.698, which was greater than 0. This indicated that the pathway was significantly upregulated in the ovaries of the CTX group (Fig. 7A). Subsequently, the interaction between Nur77 and AKT was predicted by referring to the STRING database (Fig. 7B) and using protein docking techniques (Fig. 7C). Therefore, we experimentally verified the expression of Akt/mTOR axis-related proteins in the ovarian tissues of POF mice and the changes in the expression following Nur77 overexpression. The CTX and NC-Nur77+CTX groups exhibited a significant increase in AKT and mTOR phosphorylation levels compared with the control group. However, Nur77 overexpression reversed this effect. The Akt/mTOR pathway is involved in the regulatory role of Nur77 in ovarian function (Fig. 7D and E).

Discussion

POF significantly affects women's physical and mental health [35], becoming a major public health concern to which society's attention needs to be drawn. The modern social environment is changing and has led to an increase in various environmental pollutants such as polycyclic aromatic hydrocarbons, cigarettes, aldehydes, bisphenol A, and stressors, which result in genital tumors, endocrine disorders, and ovarian dysfunction [36]. However, effective treatments are still lacking, making it crucial to explore the mechanisms underlying POF and identify new therapeutic targets.

Ideal animal models and evaluation indicators are essential for understanding mechanisms and developing drugs, with chemotherapeutic drug-induced models being a classic, simple, and common choice for POF studies [37]. Among various chemotherapeutic drugs, CTX is the most widely used for inducing POF. However, the timing and dosage of CTX used for establishing POF models vary across studies [1, 38–41]. CTX causes DNA damage-induced apoptosis within 2 days, but granulosa cell apoptosis can persist for weeks, affecting

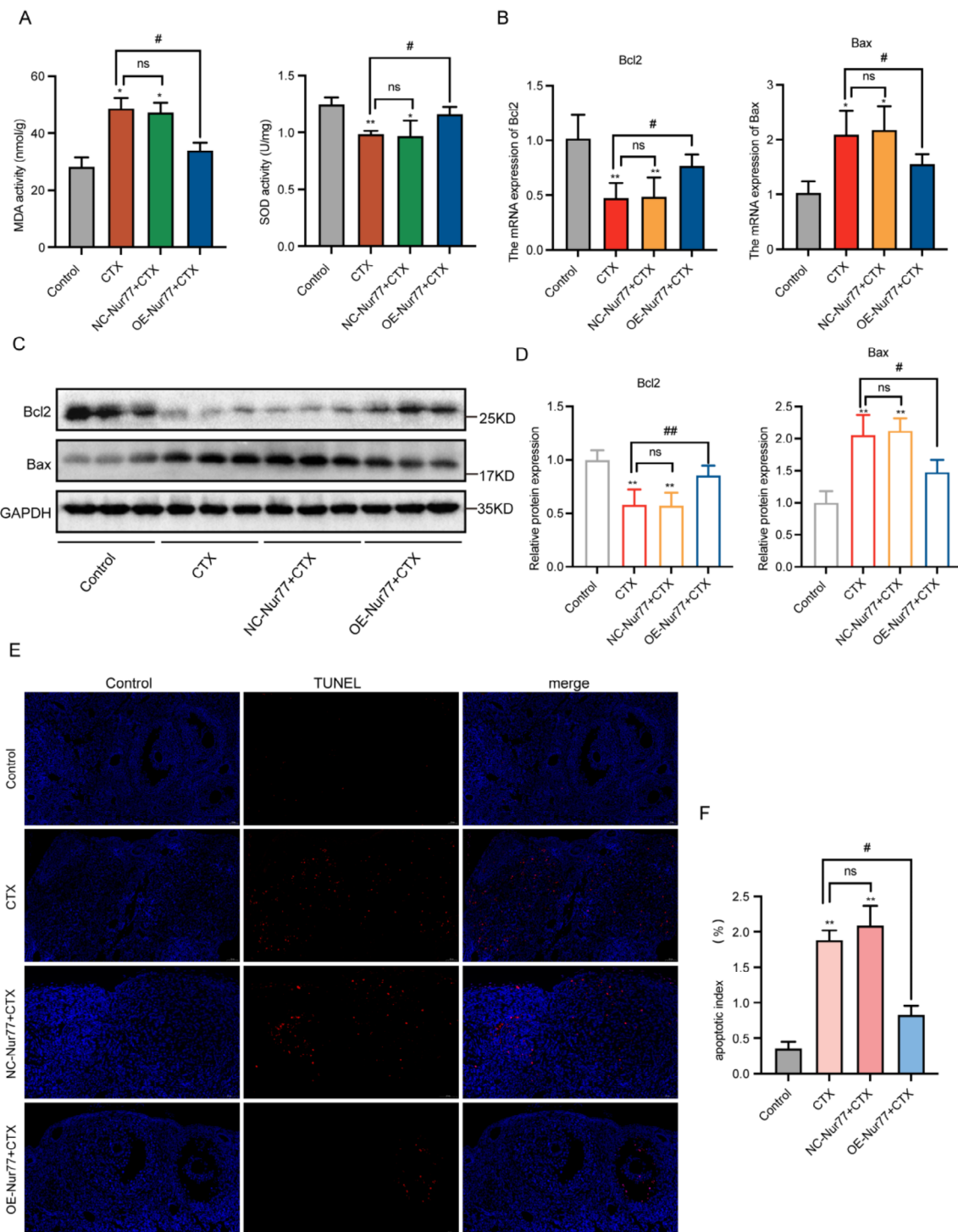


Fig. 5 Nur77 reduced oxidative stress and apoptosis in the ovaries of POF mice. **(A)** The levels of SOD and MDA in the ovarian tissues of each group after Nur77 overexpression. **(B)** The mRNA expressions of Bcl2 and Bax in each group after the overexpression of Nur77. **(C)** & **(D)** The protein expressions of Bcl2 and Bax in each group after the overexpression of Nur77. **(E)** & **(F)** Representative images of TUNEL staining of the ovaries tissues, and statistical analysis in each group after the overexpression of Nur77. Error bars, mean \pm SEM. $n=6-8/\text{group}$. * $P<0.05$, ** $P<0.01$ versus the control group. ns, not significant; # $P<0.05$, ## $P<0.01$ versus the CTX group

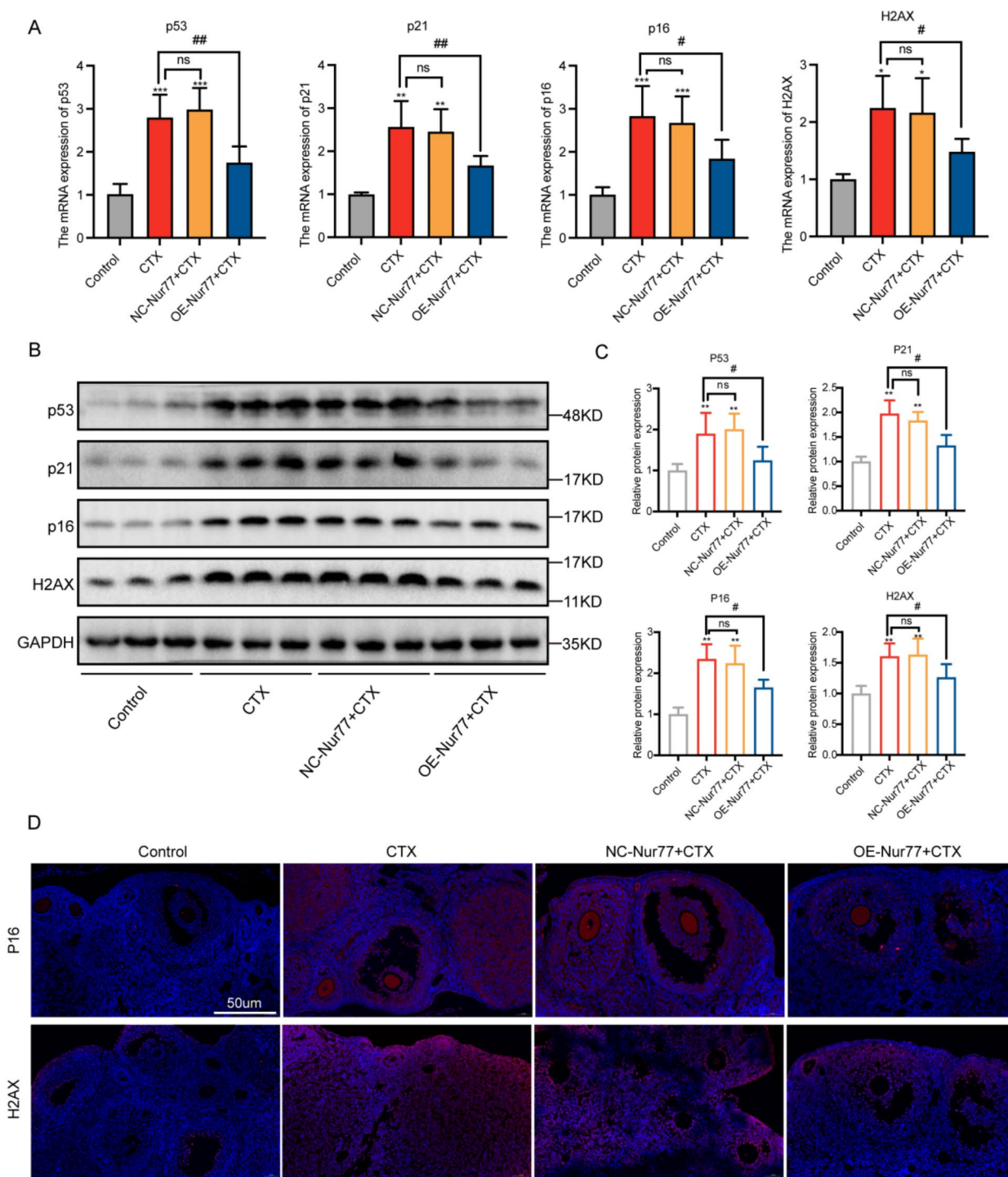


Fig. 6 Nur77 slows down ovarian aging in POF mice. **(A)** The mRNA expressions of p53, p21, p16, and H2AX in each group after overexpression of Nur77. **(B) & (C)** The protein expressions of p53, p21, p16, and H2AX in each group after the overexpression of Nur77. **(D)** Immunofluorescence staining was performed to detect the localization and expression of p16, H2AX in the ovarian tissues of each group after the overexpression of Nur77. Scale bar: 50 μ m. Error bars, mean \pm SEM. $n=6-8/\text{group}$. * $P<0.05$, ** $P<0.01$, *** $P<0.001$ versus the control group. ns, not significant; # $P<0.05$, ## $P<0.01$ versus the CTX group.

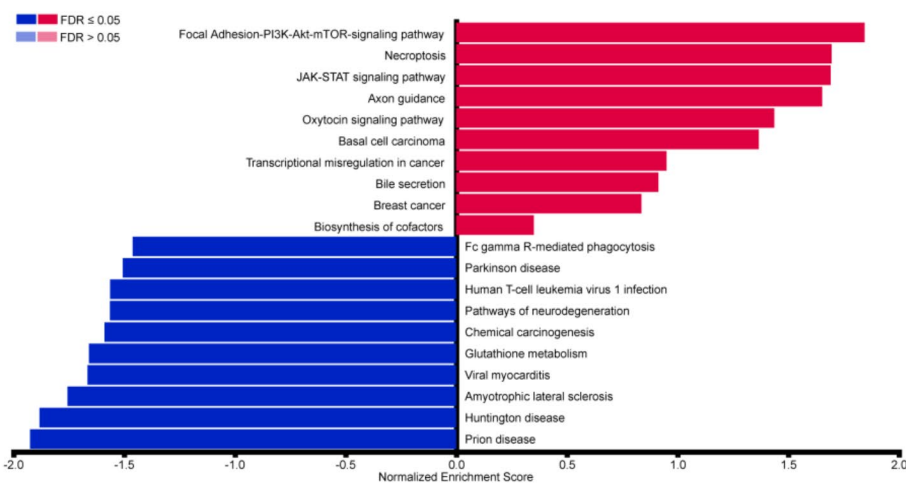
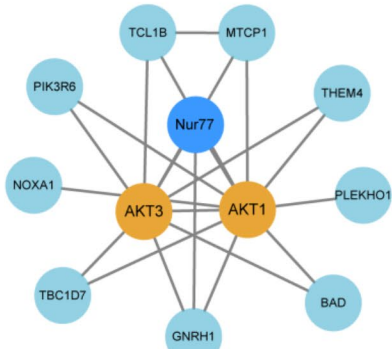
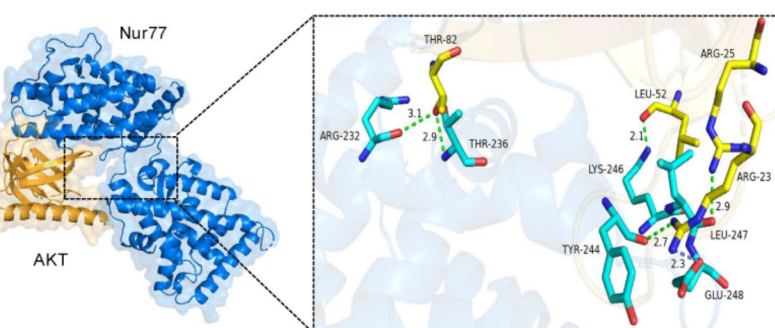
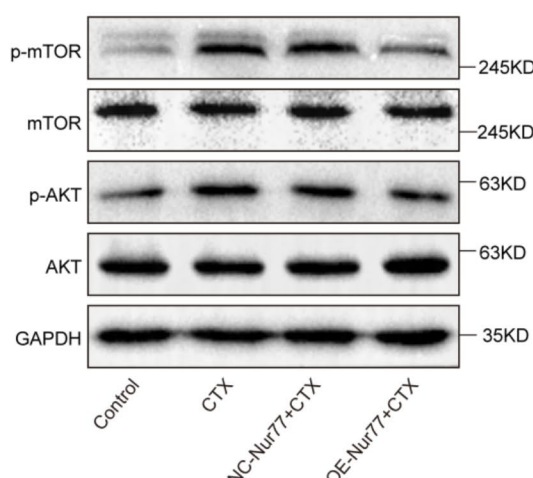
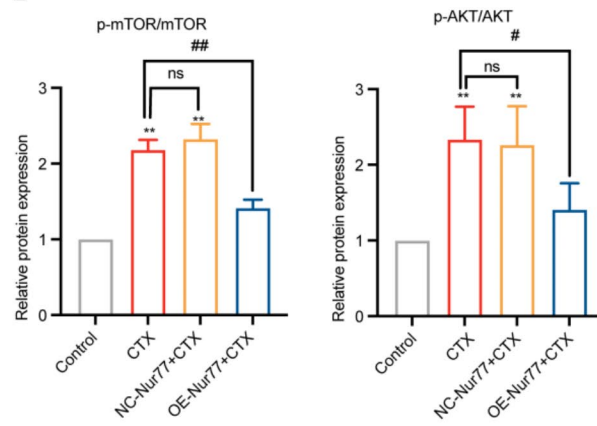
A**B****C****D****E**

Fig. 7 Nur77 improves ovarian aging in POF mice through the AKT/mTOR pathway. **(A)** The pathway enrichment analysis for the upregulated and down-regulated differentially expressed genes. **(B)** The PPI network was constructed by String, hub genes were identified. **(C)** Molecular docking analysis. Nur77 is blue, and AKT is yellow. **(D)** & **(E)** The protein expressions of p-mTOR/mTOR and p-AKT/AKT in each group after the overexpression of Nur77. Error bars, mean±SEM. $n=6-8$ /group. ** $P<0.01$ versus the control group. ns, not significant; # $P<0.05$, ## $P<0.01$ versus the CTX group

follicle growth and development. The apoptotic signals were detected even after 2 weeks of CTX administration [42]. Studies have found that 75 mg/kg CTX induces both acute (1–2 weeks after treatment) and chronic (more than 3 months) POF-like ovarian damage [1, 42, 43], making it an optimal dose. To prevent excessive damage and better comprehend Nur77 timing, we here ultimately opted for a single intraperitoneal injection of 75 mg/kg CTX to produce the POF model.

CTX causes ovarian damage not only through direct toxicity by inducing oxidative stress and apoptosis but also indirectly by depleting the ovarian reserve. CTX triggers the premature activation and excessive consumption of primordial follicles, contributing to ovarian dysfunction [44]. In our study, CTX-induced POF was characterized by abnormal sex hormone levels, including reduced AMH and E₂ levels and elevated FSH levels. AMH is known to prevent excessive activation of primordial follicles in CTX-POF mice [45, 46]. In the Nur77 overexpression group, AMH and E₂ levels increased, whereas FSH levels decreased. This indicated that Nur77 reduced the continuous loss of primordial follicles and promoted growing follicle development by restoring hormone levels. Under normal circumstances, the estrus cycle of mice changes regularly because of the action of sex hormones. The estrous cycle in the CTX group exhibited no regularity compared with that in the control group. However, the Nur77 intervention significantly improved the estrus cycle disorder.

Nur77 is an early response gene sensitive to different stimuli. It can lower oxidative damage and inflammation and preserve mitochondrial function in Parkinson's cell models and vascular endothelial dysfunction models [23, 24, 47]. However, the role of Nur77 in POF remains unclear. Therefore, we assume that Nur77 plays a protective role in CTX-induced ovarian injury. In the ovary, Nur77 overexpression significantly reversed the CTX-induced imbalance of the antioxidant index SOD and the pro-oxidation index MDA, as well as the anti-apoptotic gene Bcl2 and the pro-apoptotic gene BAX, demonstrating its potential protective role in CTX-induced ovarian injury. CTX is highly consistent in causing pathological damage to male and female reproductive functions, such as immune disorders, oxidative stress, inflammation, and apoptosis [48, 49]. At present, many studies are constantly exploring new methods for improving CTX-induced testicular injury and spermatogenic dysfunction and enhancing sperm quality [49–51]. Therefore, Nur77 could also be explored as a therapeutic target for improving chemotherapy-induced male fertility damage, warranting further investigation into its broader reproductive protective effects.

Oxidative stress, apoptosis, and aging contribute to a vicious cycle of ovarian dysfunction, particularly in the

context of CTX-induced POF. Recent in vitro and in vivo studies have indicated that CTX-POF ovaries have elevated ROS levels, telomere abnormalities, and pronounced cell senescence. This highlights the role of germ cell senescence in POF-related ovarian dysfunction [17–33]. Cell senescence is characterized by halted cell proliferation, irreversible replication arrest, and activation of tumor suppressor factors. The gene and protein expressions of the common in vitro and in vivo markers for senescent cells, namely p53, p21, p16, and H2AX [52], were significantly increased in the CTX group, confirming CTX's induction of ovarian cell senescence. Additionally, Nur77 expression, which typically declines with age in organs such as the liver and kidney, was reduced in the ovaries of the CTX-treated mice [22], as indicated by western blotting and immunofluorescence results. Because germ cell senescence and apoptosis promote follicular atresia and induce ovarian dysfunction, CTX is a drug often used for inducing POF models and determining the protective role of Nur77 in ovarian function. Nur77 overexpression countered the effects of CTX by significantly increasing the number of primordial, preantral, and antral follicles while reducing the number of atretic follicles in the CTX group, as indicated by H&E staining. However, Nur77 overexpression significantly reversed this phenomenon. Notably, Nur77 also increased corpus luteum formation, indicating that Nur77 can potentially augment ovulation. We speculate that this effect may stem from Nur77's ability to regulate various pathological stimuli and its anti-fibrotic properties [53], as evidenced by Masson staining. After Masson staining, the muscle fibers were stained red, and the collagen fibers were stained blue. This indicated that Nur77 overexpression significantly reduced the blue area in the ovaries from the CTX group. However, future studies must explore the detailed action mechanism of Nur77 in regulating CTX-induced ovarian fibrosis.

The AKT/mTOR signaling pathway is the key regulator that maintains the follicular pool, which can induce dormant follicle activation, regulate follicular growth and development, and trigger periodic ovulation [54, 55]. However, CTX can overactivate primordial follicles through the Akt/mTOR signaling pathway, leading to a "burnout" effect and follicle depletion [11, 34]. In a clinical study, changes in the expression of genes associated with the AKT/mTOR signaling pathway were evaluated in the peripheral blood of 56 control groups and 74 patients with POF through real-time fluorescence quantitative PCR. The AKT/mTOR signaling pathway was significantly activated in patients with POF [56]. In our study, the KEGG pathway enrichment unveiled that the PI3K-AKT-mTOR pathway was significantly upregulated following CTX induction. Furthermore, we predicted the interaction between Nur77 and AKT by referring to

the STRING database and through molecular docking. Therefore, we here explored whether the AKT/mTOR signaling pathway is involved in ovarian reserve regulation by Nur77. Our data revealed that AKT and mTOR phosphorylation levels were significantly increased in the CTX and NC-Nur77+CTX groups. Moreover, Nur77 overexpression decreased the activity of the AKT/mTOR pathway. The AKT/mTOR signaling pathway was involved in Nur77-mediated regulation in mouse follicles and the improvement of ovarian function.

Although Nur77 exerted a protective effect on CTX-induced ovarian injury, some limitations were observed in the present study. First, we did not continue to track birth outcomes. Additionally, immunofluorescence revealed that Nur77 expression in the follicles was elevated in the OE-Nur77+CTX group compared with the CTX group, which aligned with Nur77's role in enhancing hormone levels and follicular development. Interestingly, Nur77 expressions elevated within the ovarian stromal cells of the OE-Nur77+CTX group. An increase in the levels of fibrosis markers within ovarian stromal cells is closely linked to ovarian function decline [57]. While our study preliminary suggested that Nur77-induced improvement in ovarian function is linked to fibrosis reduction, the mechanisms through which Nur77 regulates fibrosis or improves ovarian function by targeting germ cells remain unexplored. This also highlights the study limitations and the future research direction. Single-cell sequencing has recently revealed that stromal and granulosa cells are the most prevalent cell types in the ovary [58]. Therefore, our follow-up studies will integrate in vitro and in vivo experiments to specify the germ cell types (such as oocytes, stromal cells, and granulosa cells) regulated by Nur77 and the mechanisms through which Nur77 exerts a protective effect on ovarian function.

Conclusion

In summary, although the study has limitations, it has shown that Nur77 effectively inhibits oxidative stress, aging, and apoptotic damage in CTX-POF ovaries and improves ovarian function by inhibiting the AKT/mTOR pathway. According to our results, Nur77 may be a crucial target for POF prevention and treatment.

Supplementary Information

The online version contains supplementary material available at <https://doi.org/10.1186/s13048-024-01532-y>.

Supplementary Material 1

Acknowledgements

The authors express their profound gratitude to the Experimental Animal Center of Lanzhou University for providing the equipment and space. Our appreciation also extends to the team members, without whose dedication and hard work, this study would not have been possible. We would like to

thank the staff and researchers who have contributed to data collection, analysis, and interpretation, as well as the reviewers for their valuable suggestions and comments that have greatly improved the manuscript. We also acknowledge any funding bodies that have supported this work.

Author contributions

Y.Y. and X.Z. designed and supervised the study. Y.Y. conducted the study and write the manuscript. K.Y. and B.W. raised animals, operated and collected samples. B.W. and Y.Y. performed experiments. L.W., J.S. and X.Y. performed data clean up and data analyses. Y.L., X.M. and L.W. revised the manuscript and polished the language. All authors reviewed and agreed to the final version of the manuscript.

Funding

Natural Science Foundation of Gansu Province Project (23JRRRA1617), Fund of the First Hospital of Lanzhou University (ldyyn2022-29) and Gansu Provincial Department of Education Project (2022B-015).

Data availability

No datasets were generated or analysed during the current study.

Declarations

Ethics approval and consent to participate

The research project received approval from the Ethics Review Committee of the First Hospital of Lanzhou University (Approval number: LDYLL2024-346).

Consent for publication

Not applicable.

Competing interests

The authors declare no competing interests.

Received: 5 June 2024 / Accepted: 6 October 2024

Published online: 15 October 2024

References

- Qin X, Zhao Y, Zhang T, Yin C, Qiao J, Guo W, et al. TrkB agonist antibody ameliorates fertility deficits in aged and cyclophosphamide-induced premature ovarian failure model mice. *Nat Commun*. 2022;13(1):914.
- Filippi F, Meazza C, Somigliana E, Podda M, Dallagiovanna C, Massimino M, et al. Fertility preservation in childhood and adolescent female tumor survivors. *Fertil Steril*. 2021;116(4):1087–95.
- Anthracycline-containing Taxane-containing chemotherapy for early-stage operable breast cancer: a patient-level meta-analysis of 100 000 women from 86 randomised trials. *Lancet*. 2023;401(10384):1277–92.
- Andrikopoulou A, Liantos M, Skafida E, Koutsoukos K, Apostolidou K, Kaparolou M, et al. Pembrolizumab in combination with bevacizumab and oral cyclophosphamide in heavily pre-treated platinum-resistant ovarian cancer. *Int J Gynecol Cancer*. 2023;33(4):571–76.
- Penack O, Marchetti M, Aljurf M, Arat M, Bonifazi F, Duarte RF, et al. Prophylaxis and management of graft-versus-host disease after stem-cell transplantation for haematological malignancies: updated consensus recommendations of the European Society for Blood and marrow transplantation. *Lancet Haematol*. 2024;11(2):e147–59.
- Pope JE, Denton CP, Johnson SR, Fernandez-Codina A, Hudson M, Nevskaia T. State-of-the-art evidence in the treatment of systemic sclerosis. *Nat Rev Rheumatol*. 2023;19(4):212–26.
- DeZern AE, Zahurak ML, Symons HJ, Cooke KR, Rosner GL, Gladstone DE, et al. Haploididentical BMT for severe aplastic anemia with intensive GVHD prophylaxis including posttransplant cyclophosphamide. *Blood Adv*. 2020;4(8):1770–79.
- Zheng Z, Zhang H, Peng X, Zhang C, Xing C, Xu G, et al. Effect of Tacrolimus vs Intravenous Cyclophosphamide on Complete or partial response in patients with Lupus Nephritis: a Randomized Clinical Trial. *JAMA Netw Open*. 2022;5(3):e224492.
- Szymanska KJ, Tan X, Oktay K. Unraveling the mechanisms of chemotherapy-induced damage to human primordial follicle reserve: road to developing

- therapeutics for fertility preservation and reversing ovarian aging. *Mol Hum Reprod.* 2020;26(8):553–66.
10. Trujillo M, Odle AK, Aykin-Burns N, Allen AR. Chemotherapy induced oxidative stress in the ovary: drug-dependent mechanisms and potential interventions. *Biol Reprod.* 2023;108(4):522–37.
 11. Kalich-Philosoph L, Roness H, Carmely A, Fishel-Bartal M, Ligumsky H, Paglin S, et al. Cyclophosphamide triggers follicle activation and burnout; AS101 prevents follicle loss and preserves fertility. *Sci Transl Medr.* 2013;5(185):185ra62.
 12. Oktay K, Harvey BE, Partridge AH, Quinn GP, Reinecke J, Taylor HS, et al. Fertility preservation in patients with Cancer: ASCO Clinical Practice Guideline Update. *J Clin Oncolr.* 2018;36(19):1994–2001.
 13. Zheng S, Ma M, Chen Y, Li M. Effects of quercetin on ovarian function and regulation of the ovarian PI3K/Akt/FoxO3a signalling pathway and oxidative stress in a rat model of cyclophosphamide-induced premature ovarian failure. *Basic Clin Pharmacol Toxicolr.* 2022;130(2):240–53.
 14. Ai G, Meng M, Guo J, Li C, Zhu J, Liu L, et al. Adipose-derived stem cells promote the repair of chemotherapy-induced premature ovarian failure by inhibiting granulosa cells apoptosis and senescence. *Stem Cell Res Ther.* 2023;14(1):75.
 15. Luan Y, Edmonds ME, Woodruff TK, Kim SY. Inhibitors of apoptosis protect the ovarian reserve from cyclophosphamide. *J Endocrinolr.* 2019;240(2):243–56.
 16. Barberino RS, Lins T, Monte APO, Gouveia BB, Campinho DSP, Palheta RC Jr, et al. Melatonin attenuates Cyclophosphamide-Induced primordial follicle loss by Interaction with MT(1) receptor and modulation of PTEN/Akt/FOXO3a proteins in the mouse ovary. *Reprod Scir.* 2022;29(9):2505–14.
 17. Xu Z, Takahashi N, Harada M, Kunitomi C, Kusamoto A, Koike H et al. The role of Cellular Senescence in Cyclophosphamide-Induced primary ovarian insufficiency. *Int J Mol Scir.* 2023; 24(24).
 18. Dodat F, Mader S, Lévesque D, Minireview. What is known about SUMOylation among NR4A Family members? *J Mol Biolr.* 2021;433(21):167212.
 19. Pei L, Castrillo A, Tontonoz P. Regulation of macrophage inflammatory gene expression by the orphan nuclear receptor Nur77. *Mol Endocrinolr.* 2006;20(4):786–94.
 20. Li XX, Wang ZJ, Zheng Y, Guan YF, Yang PB, Chen X, et al. Nuclear receptor Nur77 facilitates Melanoma Cell Survival under metabolic stress by protecting fatty acid oxidation. *Mol Cellr.* 2018;69(3):480–e927.
 21. Lith SC, de Vries CJM. Nuclear receptor Nur77: its role in chronic inflammatory diseases. *Essays Biochemr.* 2021;65(6):927–39.
 22. Yu Y, Song X, Wang X, Zheng L, Ma G, Liu W, et al. Oxidative stress impairs the Nur77-Sirt1 axis resulting in a decline in organism homeostasis during aging. *Aging Cellr.* 2023;22(5):e13812.
 23. Yan J, Huang J, Wu J, Fan H, Liu A, Qiao L, et al. Nur77 attenuates inflammatory responses and oxidative stress by inhibiting phosphorylated IκB-α in Parkinson's disease cell model. *Aging (Albany NY).* 2020;12(9):8107–19.
 24. Lu L, Jang S, Zhu J, Qin Q, Sun L, Sun J. Nur77 mitigates endothelial dysfunction through activation of both nitric oxide production and anti-oxidant pathways. *Redox Biolr.* 2024;70:103056.
 25. Zheng H, Liang X, Zhou H, Zhou T, Liu X, Duan J, et al. Integrated gut microbiota and fecal metabolome analyses of the effect of *Lycium barbarum* polysaccharide on D-galactose-induced premature ovarian insufficiency. *Food Functr.* 2023;14(15):7209–21.
 26. Li Q, An X, Man X, Chu M, Zhao T, Yu H, et al. Transcriptome analysis reveals that cyclophosphamide induces premature ovarian failure by blocking cholesterol biosynthesis pathway. *Life Scir.* 2019;239:116999.
 27. Geng N, Chen T, Chen L, Zhang H, Sun L, Lyu Y, et al. Nuclear receptor Nur77 protects against oxidative stress by maintaining mitochondrial homeostasis via regulating mitochondrial fission and mitophagy in smooth muscle cell. *J Mol Cell Cardiolr.* 2022;170:22–33.
 28. Chen X, Gao M, Xia Y, Wang X, Qin J, He H, et al. Phase separation of Nur77 mediates XS561-induced apoptosis by promoting the formation of Nur77/Bcl-2 condensates. *Acta Pharm Sin Br.* 2024;14(3):1204–21.
 29. Zhang T, Ma R, Li Z, Liu T, Yang S, Li N, et al. Nur77 alleviates cardiac fibrosis by upregulating GSK-3β transcription during aging. *Eur J Pharmacolr.* 2024;965:176290.
 30. Zhang S, Liu Q, Chang M, Pan Y, Yahaya BH, Liu Y, et al. Chemotherapy impairs ovarian function through excessive ROS-induced ferroptosis. *Cell Death Disr.* 2023;14(5):340.
 31. Abdool ASS, Al-Atrash AME, Soliman SS, El-Sanea AM, Gamal El Din AA, Fahmy HM. Lyophilized equine platelet-rich plasma (L-GF(equina)) antagonize the Reproductive toxicity and oxidative stress Induced by Cyclophosphamide in female rats. *J Ovarian Resr.* 2023;16(1):84.
 32. Chen H, Zhang G, Peng Y, Wu Y, Han X, Xie L, et al. Danggui Shaoyao San protects cyclophosphamide-induced premature ovarian failure by inhibiting apoptosis and oxidative stress through the regulation of the SIRT1/p53 signaling pathway. *J Ethnopharmacolr.* 2024;323:117718.
 33. Lin L, Gao W, Chen Y, Li T, Sha C, Chen L, et al. Reactive oxygen species-induced SIAH1 promotes granulosa cells' senescence in premature ovarian failure. *J Cell Mol Medr.* 2022;26(8):2417–27.
 34. Rehnitz J, Alcoba DD, Brum IS, Hinderhofer K, Youness B, Strowitzki T, et al. FM1 and AKT/mTOR signalling pathways: potential functional interactions controlling folliculogenesis in human granulosa cells. *Reprod Biomed Online.* 2017;35(5):485–93.
 35. Ishizuka B. Current understanding of the etiology, Symptomatology, and Treatment options in premature ovarian insufficiency (POI). *Front Endocrinol (Lausanne).* 2021;12:626924.
 36. Zhu X, Liu M, Dong R, Gao L, Hu J, Zhang X, et al. Mechanism exploration of environmental pollutants on premature ovarian insufficiency: a systematic review and Meta-analysis. *Reprod Scir.* 2024;31(1):99–106.
 37. Dai F, Wang R, Deng Z, Yang D, Wang L, Wu M, et al. Comparison of the different animal modeling and therapy methods of premature ovarian failure in animal model. *Stem Cell Res Ther.* 2023;14(1):135.
 38. Chen Y, Zhao Y, Miao C, Yang L, Wang R, Chen B, et al. Quercetin alleviates cyclophosphamide-induced premature ovarian insufficiency in mice by reducing mitochondrial oxidative stress and pyroptosis in granulosa cells. *J Ovarian Resr.* 2022;15(1):138.
 39. Ma H, Wang Y, Liu G, Hu Q, Zhu J, Dai Y. Ovarian scaffolds promoted mouse ovary recovery from cyclophosphamide damage. *J Reprod Immunolr.* 2023;157:103950.
 40. Liu X, Song Y, Zhou F, Zhang C, Li F, Hu R, et al. Network and experimental pharmacology on mechanism of Si-Wu-tang improving ovarian function in a mouse model of premature ovarian failure induced by cyclophosphamide. *J Ethnopharmacolr.* 2023;301:115842.
 41. Mattiello L, Pucci G, Marchetti F, Diederich M, Gonfloni S. Asciminib mitigates DNA damage stress Signaling Induced by Cyclophosphamide in the Ovary. *Int J Mol Scir.* 2021; 22(3).
 42. Pascual N, Scotti L, Di Pietro M, Oubiña G, Bas D, May M, et al. Ceramide-1-phosphate has protective properties against cyclophosphamide-induced ovarian damage in a mice model of premature ovarian failure. *Hum Reprod.* 2018;33(5):844–59.
 43. Meirow D, Lewis H, Nugent D, Epstein M. Subclinical depletion of primordial follicular reserve in mice treated with cyclophosphamide: clinical importance and proposed accurate investigative tool. *Hum Reprod.* 1999;14(7):1903–7.
 44. Bhardwaj JK, Bikal P, Sachdeva SN. Chemotherapeutic drugs induced female reproductive toxicity and treatment strategies. *J Biochem Mol Toxicolr.* 2023;37(7):e23371.
 45. Sonigo C, Beau I, Grynberg M, Binart N. AMH prevents primordial ovarian follicle loss and fertility alteration in cyclophosphamide-treated mice. *Faseb Jr.* 2019;33(1):1278–87.
 46. Rosario R, Stewart HL, Spears N, Telfer EE, Anderson RA. Anti-mullerian hormone attenuates both cyclophosphamide-induced damage and PI3K signalling activation, while rapamycin attenuates only PI3K signalling activation, in human ovarian cortex in vitro. *Hum Reprod.* 2024;39(2):382–92.
 47. Peng SZ, Chen XH, Chen SJ, Zhang J, Wang CY, Liu WR, et al. Phase separation of Nur77 mediates celastrol-induced mitophagy by promoting the liquidity of p62/SQSTM1 condensates. *Nat Communr.* 2021;12(1):5989.
 48. Fani F, Hosseiniemehr SJ, Zargari M, Mirzaei M, Karimpour Malekshah A, Talebpour Amiri F. Piperine mitigates oxidative stress, inflammation, and apoptosis in the testicular damage induced by cyclophosphamide in mice. *J Biochem Mol Toxicolr.* 2024;38(4):e23696.
 49. Tian B, Jiang Y, Liu R, Hamed YS, Rayan AM, Xu S, et al. Positive effects of extracellular polysaccharides from *Paeciliomyces heipali* on immune-enhancing properties by regulating gut microbiota in cyclophosphamide-induced mice. *Int J Biol Macromolr.* 2024;274(Pt 2):133390.
 50. Ye Y, Fang C, Li L, Liu D, Wang Y, Huang F, et al. Protective effect of L-Theanine on Cyclophosphamide-Induced Testicular toxicity in mice. *J Agric Food Chemr.* 2023;71(21):8050–60.
 51. Zhao Y, Wu J, Li X, Chen Q, Hong Z, Zheng L, et al. Protective effect of Huangqi-Guizhi-Wuwtang against cyclophosphamide-induced spermatogenesis dysfunction in mice by promoting steroid hormone biosynthesis. *J Ethnopharmacolr.* 2024;319(Pt 2):117260.
 52. Ogrordnik M. Cellular aging beyond cellular senescence: markers of senescence prior to cell cycle arrest in vitro and in vivo. *Aging Cellr.* 2021;20(4):e13338.

53. Ma G, Chen F, Liu Y, Zheng L, Jiang X, Tian H, et al. Nur77 ameliorates age-related renal tubulointerstitial fibrosis by suppressing the TGF- β /Smads signaling pathway. *Faseb Jr.* 2022;36(2):e22124.
54. Hsueh AJ, Kawamura K, Cheng Y, Fauser BC. Intraovarian control of early folliculogenesis. *Endocr Rev.* 2015;36(1):1–24.
55. Makker A, Goel MM, Mahdi AA. PI3K/PTEN/Akt and TSC/mTOR signaling pathways, ovarian dysfunction, and infertility: an update. *J Mol Endocrinol.* 2014;153(3):R103–18.
56. Rehnitz J, Messmer B, Bender U, Nguyen XP, Germeyn A, Hinderhofer K, et al. Activation of AKT/mammalian target of rapamycin signaling in the peripheral blood of women with premature ovarian insufficiency and its correlation with FMR1 expression. *Reprod Biol Endocrinol.* 2022;20(1):44.
57. Cui L, Bao H, Liu Z, Man X, Liu H, Hou Y, et al. hUMSCs regulate the differentiation of ovarian stromal cells via TGF- β (1)/Smad3 signaling pathway to inhibit ovarian fibrosis to repair ovarian function in POI rats. *Stem Cell Res Ther.* 2020;11(1):386.
58. Isola JV, Ocañas SR, Hubbard CR, Ko S, Mondal SA, Hense JD, et al. A single-cell atlas of the aging mouse ovary. *Nat Agingr.* 2024;4(1):145–62.

Publisher's note

Springer Nature remains neutral with regard to jurisdictional claims in published maps and institutional affiliations.